Supplementary Information

wALADin benzimidazoles differentially modulate the function of porphobilinogen synthase orthologs

*Christian S. Lentz[†], Victoria S. Halls[‡], Jeffrey Hannam[‡], Silke Strassel[†], Sarah H. Lawrence[□], Eileen K. Jaffe[□], Michael Famulok[‡], Achim Hoerauf[†], Kenneth M. Pfarr[†]**

[†] Institute of Medical Microbiology, Immunology and Parasitology, University Hospital of Bonn, Sigmund-Freud Str. 25, 53127 Bonn, Germany

[‡] LIMES Institute, Chemical Biology & Medicinal Chemistry Unit, University of Bonn, Gerhard-Domagk-Str. 1, 53121 Bonn, Germany

[□] Fox Chase Cancer Center, Temple University Health System, 333 Cottman Ave, Philadelphia, PA, 19111 USA.

Contents:

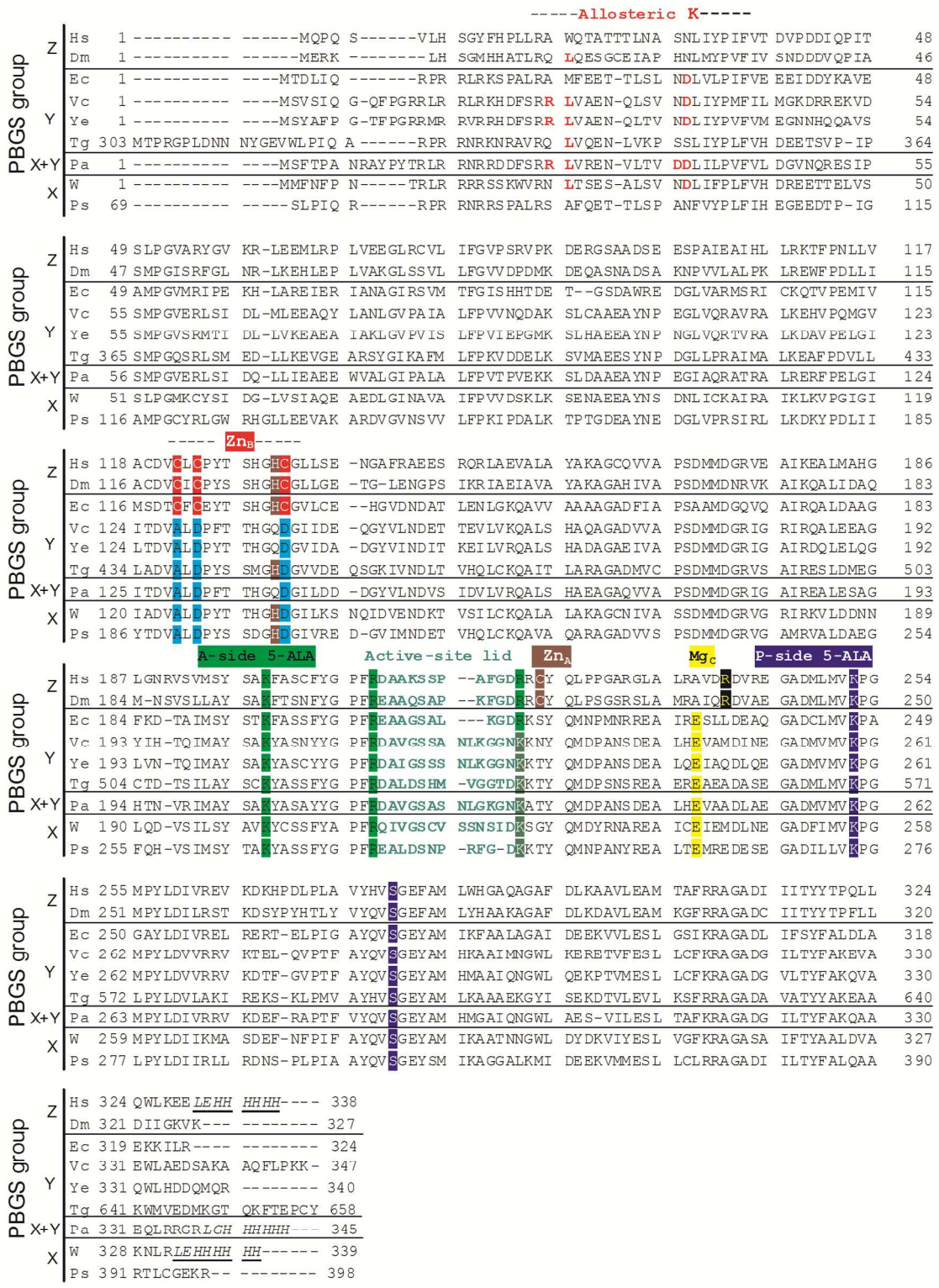
-----Allosteric K-----
PBGS group
Z
Y
X+Y
X
Hs 1 ---------- ------MQPQ S------VLH SGYFHPLLRA WQTATTTLNA SNLIYPIFVT DVPDDIQPIT 48
Dm 1 ---------- ------MERK --------LH SGMHHATLRQ LQESGCEIAP HNLMYPVFIV SNDDDVQPIA 46
Ec 1 ---------- ----MTDLIQ -------RPR RLRKSPALRA MFEET-TLSL NDLVLPIFVE EEIDDYKAVE 48
Vc 1 ---------- ----MSVSIQ G-QFPGRRLR RLRKHDFSRR LVAEN-QLSV NDLIYPMFIL MGKDRREKVD 54
Ye 1 ---------- ----MSYAFP G-TFPGRRMR RVRRHDFSRR LVAEN-QLTV NDLIYPVFVM EGNNHQQAVS 54
Tg 303 MTPRGPLDNN NYGEVWLPIQ A------RPR RNRKNRAVRQ LVQEN-LVKP SSLIYPLFVH DEETSVP-IP 364
Pa 1 ---------- ----MSFTPA NRAYPYTRLR RNRRDDFSRR LVREN-VLTV DDLILPVFVL DGVNQRESIP 55
W 1 ---------- ----MMFNFP N-----TRLR RRRSSKWVRN LTSES-ALSV NDLIFPLFVH DREETTELVS 50
Ps 69 ---------- -----SLPIQ R------RPR RNRRSPALRS AFQET-TLSP ANFVYPLFIH EGEEDTP-IG 115
Hs 49 SLPGVARYGV KR-LEEMLRP LVEEGLRCVL IFGVPSRVPK DERGSAADSE ESPAIEAIHL LRKTFPNLLV 117
Dm 47 SMPGISRFGL NR-LKEHLEP LVAKGLSSVL LFGVVDPDMK DEQASNADSA KNPVVLALPK LREWFPDLLI 115
Ec 49 AMPGVMRIPE KH-LAREIER IANAGIRSVM TFGISHHTDE T--GSDAWRE DGLVARMSRI CKQTVPEMIV 115
Vc 55 SMPGVERLSI DL-MLEEAQY LANLGVPAIA LFPVVNQDAK SLCAAEAYNP EGLVQRAVRA LKEHVPQMGV 123
Ye 55 SMPGVSRMTI DL-LVKEAEA IAKLGVPVIS LFPVIEPGMK SLHAEEAYNP NGLVQRTVRA LKDAVPELGI 123
Tg 365 SMPGQSRLSM ED-LLKEVGE ARSYGIKAFM LFPKVDDELK SVMAEESYNP DGLLPRAIMA LKEAFPDVLL 433
Pa 56 SMPGVERLSI DQ-LLIEAEE WVALGIPALA LFPVTPVEKK SLDAAEAYNP EGIAQRATRA LRERFPELGI 124
W 51 SLPGMKCYSI DG-LVSIAQE AEDLGINAVA IFPVVDSKLK SENAEEAYNS DNLICKAIRA IKLKVPGIGI 119
Ps 116 AMPGCYRLGW RHGLLEEVAK ARDVGVNSVV LFPKIPDALK TPTGDEAYNE DGLVPRSIRL LKDKYPDLII 185
----- Zn_B -----
Hs 118 ACDVCLCPYT SHGHCGLLSE -NGAFRAEES RQRLAEVALA YAKAGCQVVA PSDMMDGRVE AIKEALMAHG 186
Dm 116 ACDVCICPYS SHGHCGLLGE -TG-LENGPS IKRIAEIAVA YAKAGAHIVA PSDMMDNRVK AIKQALIDAQ 183
Ec 116 MSDTCFCEYT SHGHCGVLCE --HGVDNDAT LENLGKQAVV AAAAGADFIA PSAAMDGQVQ AIRQALDAAG 183
Vc 124 ITDVALDPFT THGQDGIIDE -QGYVLNDET TEVLVKQALS HAQAGADVVA PSDMMDGRIG RIRQALEEAG 192
Ye 124 LTDVALDPYT THGQDGVIDA -DGYVINDIT KEILVRQALS HADAGAEIVA PSDMMDGRIG AIRDQLELQG 192
Tg 434 LADVALDPYS SMGHDGVVDE QSGKIVNDLT VHQLCKQAIT LARAGADMVC PSDMMDGRVS AIRESLDMEG 503
Pa 125 ITDVALDPFT THGQDGILDD -DGYVLNDVS IDVLVRQALS HAEAGAQVVA PSDMMDGRIG AIREALESAG 193
W 120 IADVALDPYT THGHDGILKS NQIDVENDKT VSILCKQALA LAKAGCNIVA SSDMMDGRVG RIRKVLDDNN 189
Ps 186 YTDVALDPYS SDGHDGIVRE D-GVIMNDET VHQLCKQAVA QARAGADVVS PSDMMDGRVG AMRVALDAEG 254
A-side 5-ALA
Active-site lid
Zn_A
Mg_C
P-side 5-ALA
Hs 187 LGNRVSVMSY SAKFASCFYG PFRDAAKSSP --AFGDERCY QLPPGARGLA LRAVDRDVRE GADMLMVKPG 254
Dm 184 M-NSVSLLAY SAKFTSNFYG PFREAAQSAP --KFGDERCY QLPSGSRSLA MRAIQRDVAE GADMLMVKPG 250
Ec 184 FKD-TAIMSY STKFASSFYG PFREAAGSAL ---KGDEKSY QMNPMNRREA IRESLLDEAQ GADCLMVKPA 249
Vc 193 YIH-TQIMAY SAKYASNYYG PFRDAVGSSA NLKGGNKKNY QMDPANSDEA LHEVAMDINE GADMVMVKPG 261
Ye 193 LVN-TQIMAY SAKYASCYYG PFRDAIGSSS NLKGGNKKTY QMDPANSDEA LQEIAQDLQE GADMVMVKPG 261
Tg 504 CTD-TSILAY SCKYASSFYG PFRDALDSHM -VGGTDKKTY QMDPSNSREA EREAEADASE GADMLMVKPG 571
Pa 194 HTN-VRIMAY SAKYASAYYG PFRDAVGSAS NLGKGNKATY QMDPANSDEA LHEVAADLAE GADMVMVKPG 262
W 190 LQD-VSILSY AVKYCSSFYA PFRQIVGSCV SSNSIDKSGY QMDYRNAREA ICEIEMDLNE GADFIMVKPG 258
Ps 255 FQH-VSIMSY TAKYASSFYG PFREALDSNP -RFG-DKKTY QMNPANYREA LTEMREDESE GADILLVKPG 276
Hs 255 MPYLDIVREV KDKHPDLPLA VYHVSGEFAM LWHGAQAGAF DLKAAVLEAM TAFRRAGADI IITYYTPQLL 324
Dm 251 MPYLDILRST KDSYPYHTLY VYQVSGEFAM LYHAAKAGAF DLKDAVLEAM KGFRRAGADC IITYYTPFLL 320
Ec 250 GAYLDIVREL RERT-ELPIG AYQVSGEYAM IKFAALAGAI DEEKVVLESL GSIKRAGADL IFSYFALDLA 318
Vc 262 MPYLDVVRRV KTEL-QVPTF AYQVSGEYAM HKAAIMNGWL KERETVFESL LCFKRAGADG ILTYFAKEVA 330
Ye 262 MPYLDVVRRV KDTF-GVPTF AYQVSGEYAM HMAAIQNGWL QEKPTVMESL LCFKRAGADG VLTYFAKQVA 330
Tg 572 LPYLDVLAKI REKS-KLPMV AYHVSGEYAM LKAAAEKGYI SEKDTVLEVL KSFRRAGADA VATYYAKEAA 640
Pa 263 MPYLDIVRRV KDEF-RAPTF VYQVSGEYAM HMGAIQNGWL AES-VILESL TAFKRAGADG ILTYFAKQAA 330
W 259 MPYLDIIKMA SDEF-NFPIF AYQVSGEYAM IKAATNNGWL DYDKVIYESL VGFKRAGASA IFTYAALDVA 327
Ps 277 LPYLDIIRLL RDNS-PLPIA AYQVSGEYSM IKAGGALKMI DEEKVMMESL LCLRRAGADI ILTYFALQAA 390
Hs 324 QWLKEELEHH HHHH---- 338
Dm 321 DIIGKVK--- -------- 327
Ec 319 EKKILR---- -------- 324
Vc 331 EWLAEDSAKA AQFLPKK- 347
Ye 331 QWLHDDQMQR -------- 340
Tg 641 KWMVEDMKGT QKFTEPCY 658
Pa 331 EQLRRGRLGH HHHHH--- 345
W 328 KNLRLEHHHH HH------ 339
Ps 391 RTLCGEKR-- -------- 398

Figure S1. Multiple Sequence Alignment of orthologous protein sequences of *Homo sapiens* (Hs, Uniprot ID P13716), *Drosophila melanogaster* (Dm, Q9VTV9*), Escherichia coli* (Ec; P0ACB2), *Vibrio cholerae* (Vc; C3LPU7)), *Pseudomonas aeruginosa* (Pa; Q59643), *Yersinia enterocolitica* (Ye; F4MUJ9), *Toxoplasma gondii* (Tg; B6KNM2), *Wolbachia* of *Brugia malayi* (W; Q5GSR3) and *Pisum sativum* (Ps; P30124) PBGS by ClustalW implemented W in GENtle V 1.9.4 (Magnus Manske, Cologne, 2003) using a BLOSUM matrix and the following scores: Match: 2; Gap external penalty: -1; Gap penalty: -2. The N-terminal sequence chloroplast targeting sequence of *Ps*PBGS (amino acids 1 - 68) and the apicoplast targeting sequence and low complexity region (amino acids 1 – 302) of *Tg*PBGS were excluded from the respective recombinant proteins. C-terminal tags of recombinant proteins are underlined and italicized, if present. Important structural features are highlighted: Binding site for allosteric K^+ (red font, full motif according to *Pa*PBGS), Catalytic Zn_B^{2+}-site (red), the alternative motif of Zn^{2+}-independent orthologs (cyan), Zn_A^{2+}-site (brown), binding site for A-side 5-ALA (i.e. the 5-ALA giving rise to the **A**cetyl moiety in porphobilinogen, green), binding site for P-side 5-ALA (i.e. the 5-ALA giving rise to the **P**ropionyl moiety in porphobilinogen, blue), active site lid (green font), the allosteric Mg_C binding site (yellow) or the characteristic arginine residue of non Mg^{2+}-responsive orthologs (yellow font on black background). Orthologous PBGS protein sequences were aligned in a multiple sequence alignment with Clustal

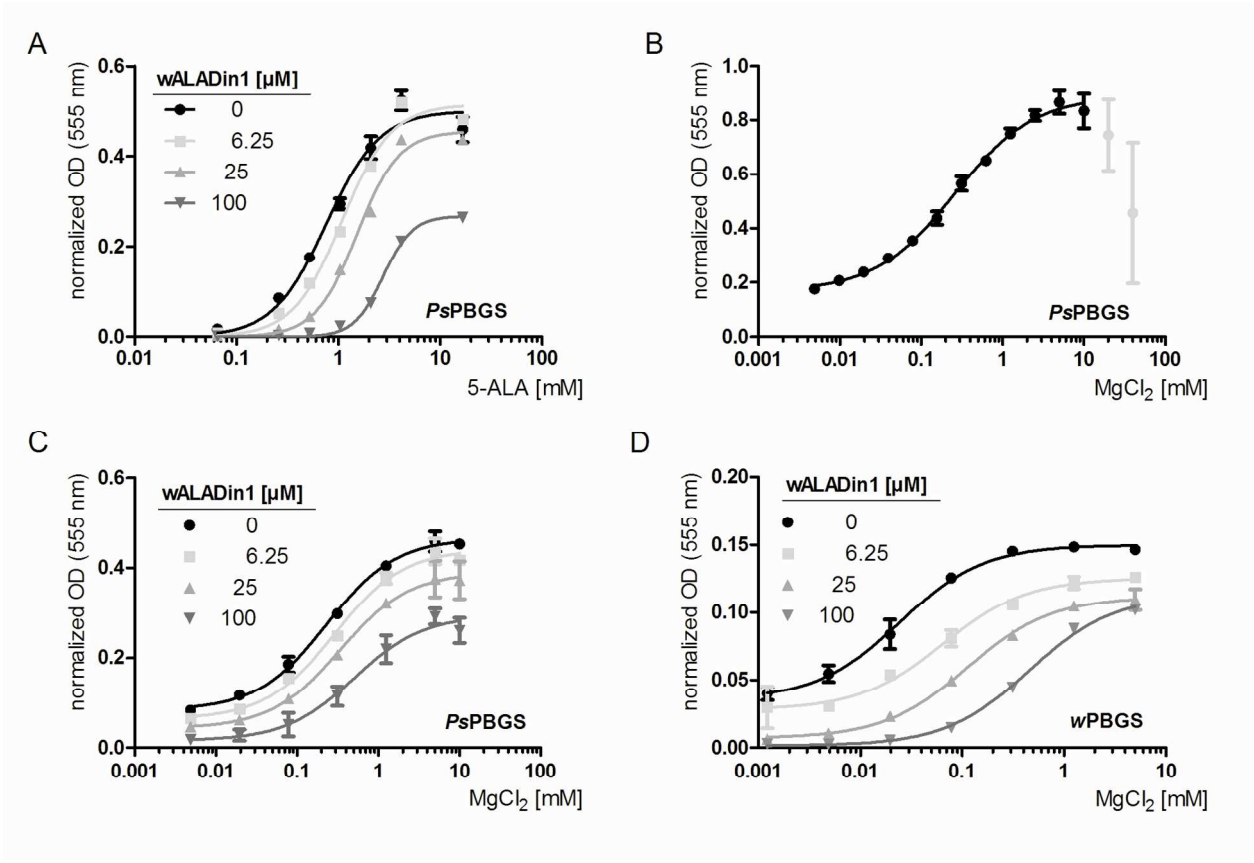

Figure S2. Inhibition of *Ps*PBGS and *w*PBGS by wALADin1. A) Substrate-concentration series of *Ps*PBGS in the presence of increasing concentrations of wALADin1. Curves were fit assuming an "Allosteric sigmoidal" model using Prism 5.0 software ($Y=V_{MAX}*X^h/(K' + X^h)$ with K' being related but not identical to K_M, unless h = 1). A reduction in V_{MAX} and an increase in K' are consistent with a mixed competitive/noncompetitive model of inhibition. Hill slopes were as follows: 1.665 (0 µM wALADin1); 1.795 (6.25 µM wALADin1); 2.111 (25 µM wALADin1); 3.020 (100 µM wALADin1). B) Mg^{2+}-response curve of *Ps*PBGS with a $K_{0.5}$ of ~ 257 µM at a saturating 5-ALA concentration of 10 mM. High inhibitory Mg^{2+} concentrations (depicted in grey were excluded from non-linear regression analysis. C) wALADin1 reduced the affinity for Mg^{2+} and decreased the maximum activity achieved by stimulation of *Ps*PBGS by $Mg^{2+}$and D) *w*PBGS. Graphs B - D were fit to a sigmoidal four parameter non-linear regression

model. For *w*PBGS the decrease in affinity to Mg^{2+} was nearly 10-fold more pronounced than for *Ps*PBGS (18.6–fold vs. 2.2-fold increase of $K_{0.5}$ at 100 µM wALADin1, respectively). *Ps*PBGS was assayed at 300 nM in 100 mM BTP-HCl pH 8.5, 1 mM $MgCl_2$, 5 mM DTT for 15 min, *w*PBGS at 500 nM in 100 mM Tris-HCl pH 8.0, 1 mM $MgCl_2$, 5 mM DTT, if not indicated otherwise. Graphs show means ± SD of triplicates and are representative of 2 independent experiments.

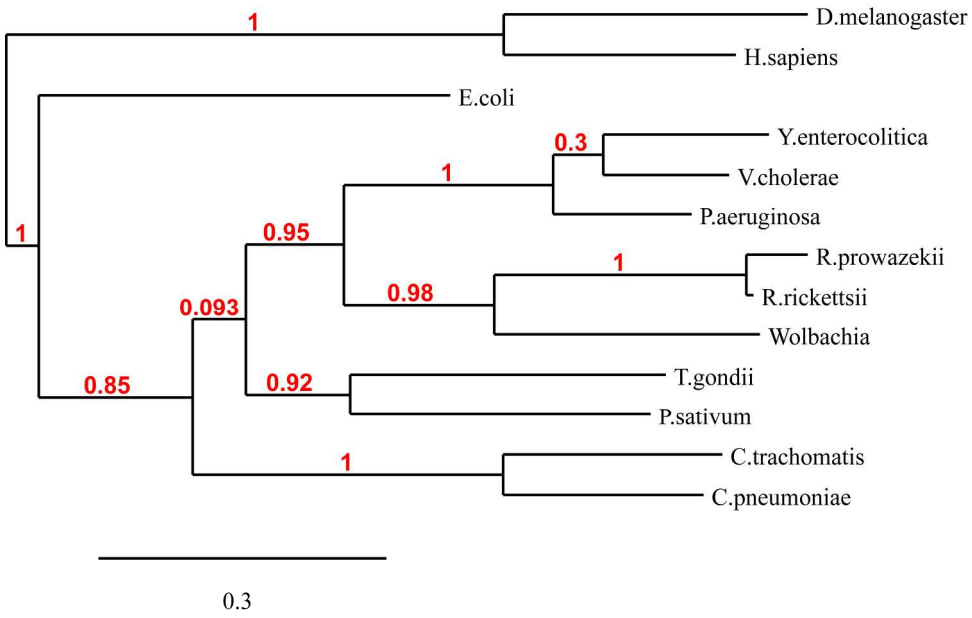

Figure S3. Phylogeny of PBGS. The tree was created using alignment, curation, phylogeny and tree rendering programs integrated into the website www.phylogeny.fr. [1, 2] Input sequences were: *V. cholerae* (UniProtKB C3LPU7), *Y. enterocolitica* (F4MUJ9), *E. coli* (P0ACB2), *D. melanogaster* (Q9VTV9), *P. sativum* (P30124), *T. gondii* (B6KNM2), *H. sapiens* (P13716), *Wolbachia* of *B. malayi* (Q5GSR3). In addition, PBGS sequences from the obligate intracellular bacteria *Rickettsia rickettsii* (B0BY42), *R. prowazekii* (Q9ZD11), *Chlamydia pneumoniae* (Q9Z7G1) and *C. trachomatis* (O84638) were entered. The initial multiple sequence alignment was done using MUSCLE [3] (v. 3.7) using default settings. Gblock[4] (v091.b) was used to remove

ambiguous regions (Settings: Minimum sequences for flank position: 85%; Maximum contiguous nonconserved positions: 8; Minimum block length: 10; Gaps in final blocks: no). The phylogenetic tree was created using a maximum likelihood method implemented in PhyML[5, 6] (*v3.0 aRLT*) (Settings: Model: WAG; Statistical test: alrt; Number of categories: 4; Gamma: estimated; Invariable sites: estimated; Remove gaps: enabled). The graphical representation of the tree was done with TreeDyn[7] (*v198.3*). The red numbers indicate branch support values, the branch length scale is shown in black.

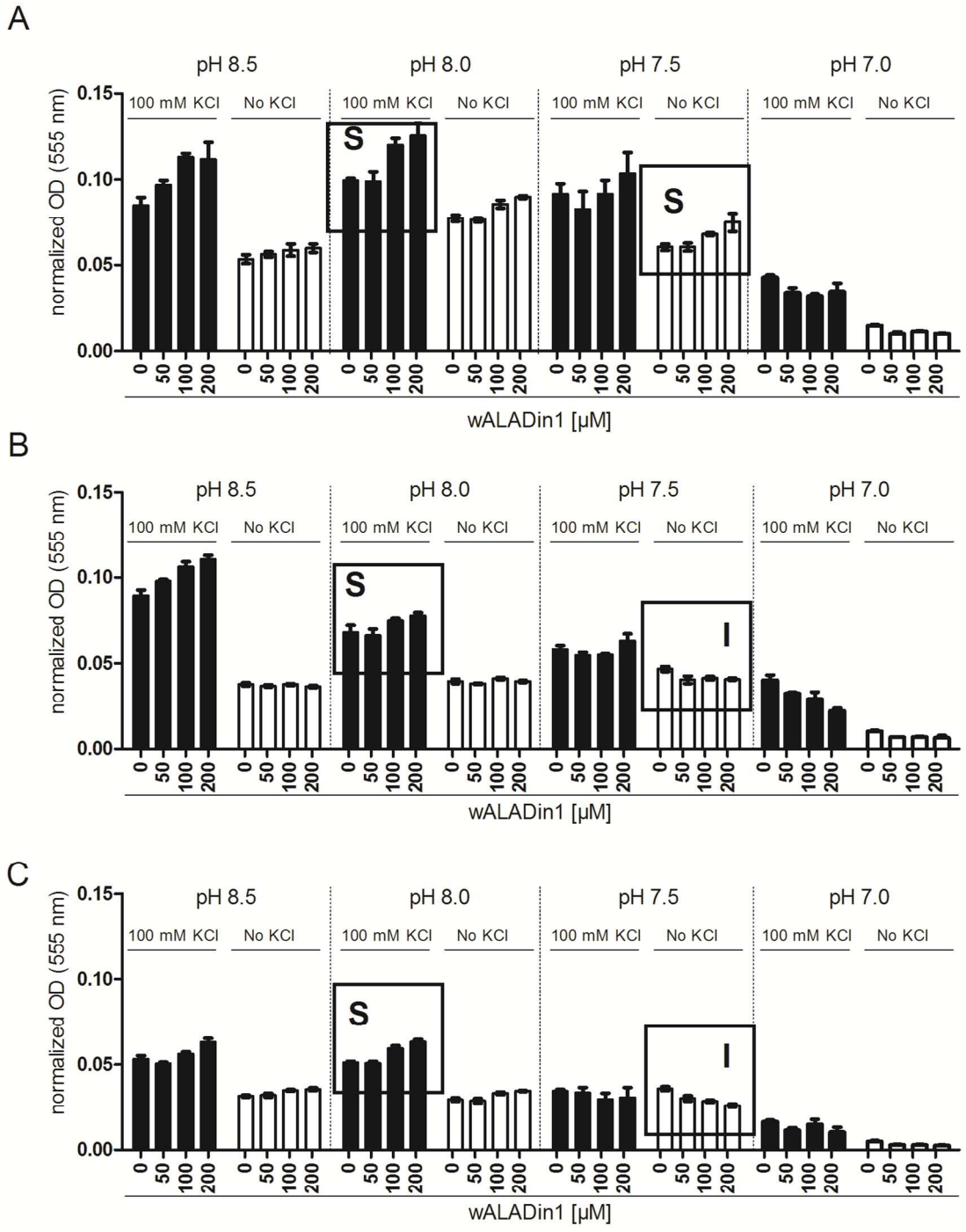

Figure S4. The effect of KCl, pH, and [5-ALA] on wALADin1 activity against *Pseudomonas aeruginosa* PBGS. A) Saturating 5-ALA concentration: 5 mM. B) Near-saturating 5-ALA concentration: 1 mM. C) Non-saturating 5-ALA concentration: 200 μM. Closed bars: 100 mM KCl; open bars: no KCl. Boxes with "S" mark conditions under which the stimulatory effect of

wALADin1 on *Pa*PBGS was most pronounced, boxes with "I" mark conditions with strong inhibitory effects.

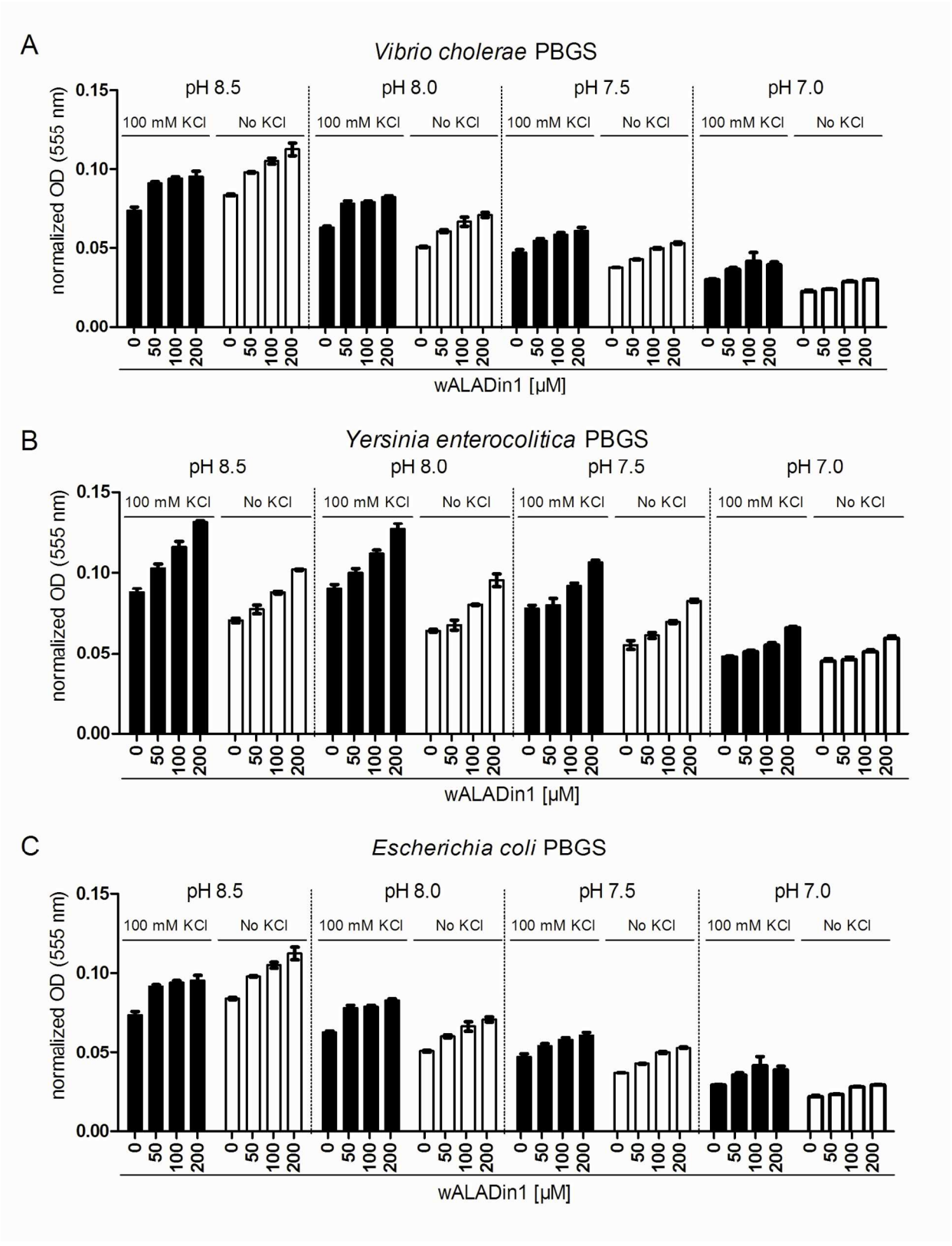
A
Vibrio cholerae PBGS
pH 8.5
pH 8.0
pH 7.5
pH 7.0
100 mM KCl
No KCl
normalized OD (555 nm)
0.15
0.10
0.05
0.00
0
50
100
200
wALADin1 [µM]
B
Yersinia enterocolitica PBGS
C
Escherichia coli PBGS

Figure S5. pH screen of stimulated *Vc*, *Ye* and *Ec*PBGS orthologs: A) *Vibrio cholerae* PBGS (125 nM); B) *Yersinia enterocolitica* PBGS (150 nM); C) *Escherichia coli* PBGS (200 nM). wALADin1 acted in a stimulatory fashion under all conditions tested. For all orthologs enzymatic assays were carried out in 100 mM BTP-HCl, 1 mM $MgCl_2$, 5 mM DTT and 200 µM 5-ALA for 10 min. *Ec*PBGS contained 10 µM $ZnCl_2$. Graphs show means ± SD of triplicates.

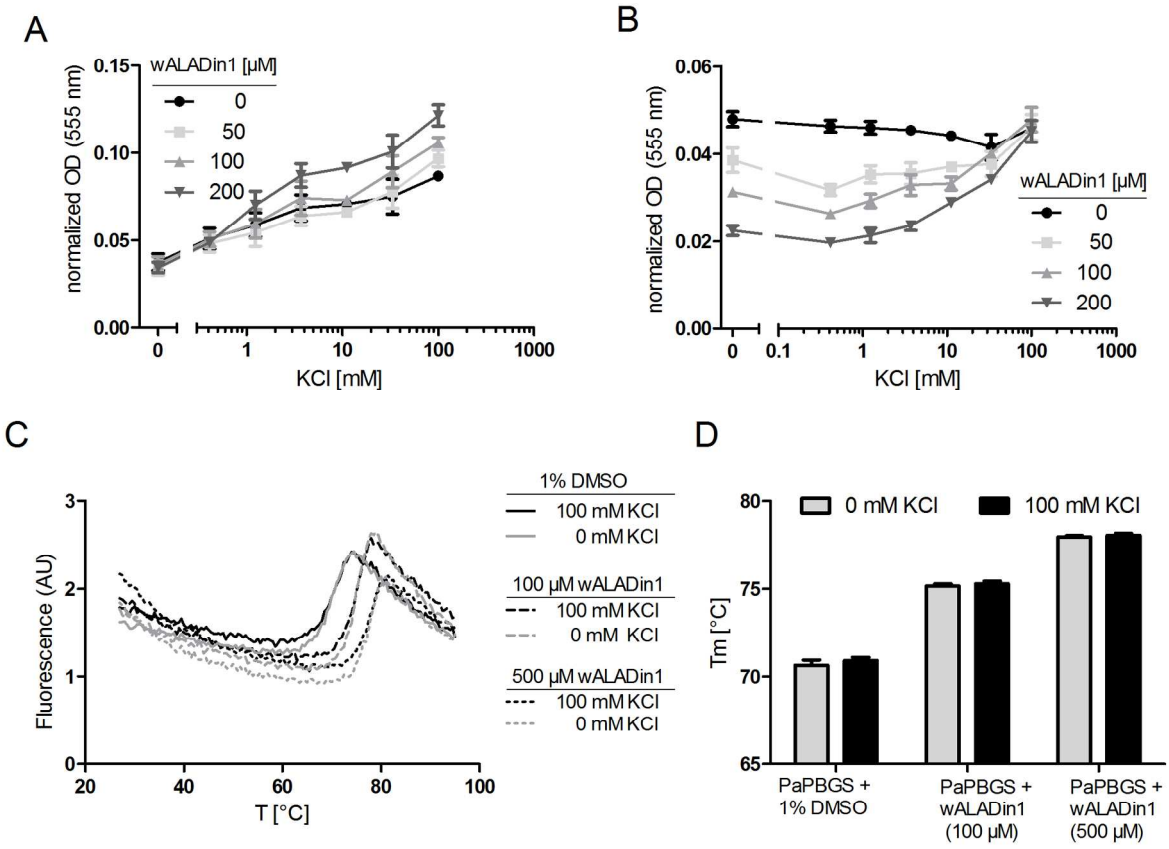

Figure S6. The effect of K^+ on the interaction of *Pa*PBGS and wALADin1. (A), (B) Effect of K^+ dilution series on *Pa*PBGS activity under the influence of wALADin1. A) While in the absence of K^+ no stimulatory activity of wALADin1 is observed, at high [KCl] wALADin1 stimulated PaPBGS activity (standard stimulatory conditions: 100 mM Tris-HCl pH 8.0, 5 mM 5-ALA, 1 mM $MgCl_2$),. B) In contrast, under "standard inhibitory" conditions (100 mM Tris-HCl pH 7.5, 0.2 mM 5-ALA, 1 mM $MgCl_2$) high [KCl] counteracted the inhibitory effect of wALADin1. (A)

and (B) show means ± SD of triplicates and are representative of two experiments. (C), (D) Protein thermal shift assay of *Pa*PBGS. A) Melting curve of *Pa*PBGS monitored as an increase in Sypro® Orange fluorescence bound to denatured protein. (B) Melting temperature (T_m) of *Pa*PBGS under the different conditions. KCl had no influence on the melting temperature in the presence or absence of wALADin1. 5 µM *Pa*PBGS was incubated in 100 mM Tris-HCl pH 8.0, 10 mM MgCl2, and 8X Sypro® Orange in the presence or absence of 100 mM KCl with 1% DMSO, and 100 µM or 500 µM wALADin1. The graphs are representative of two experiments.

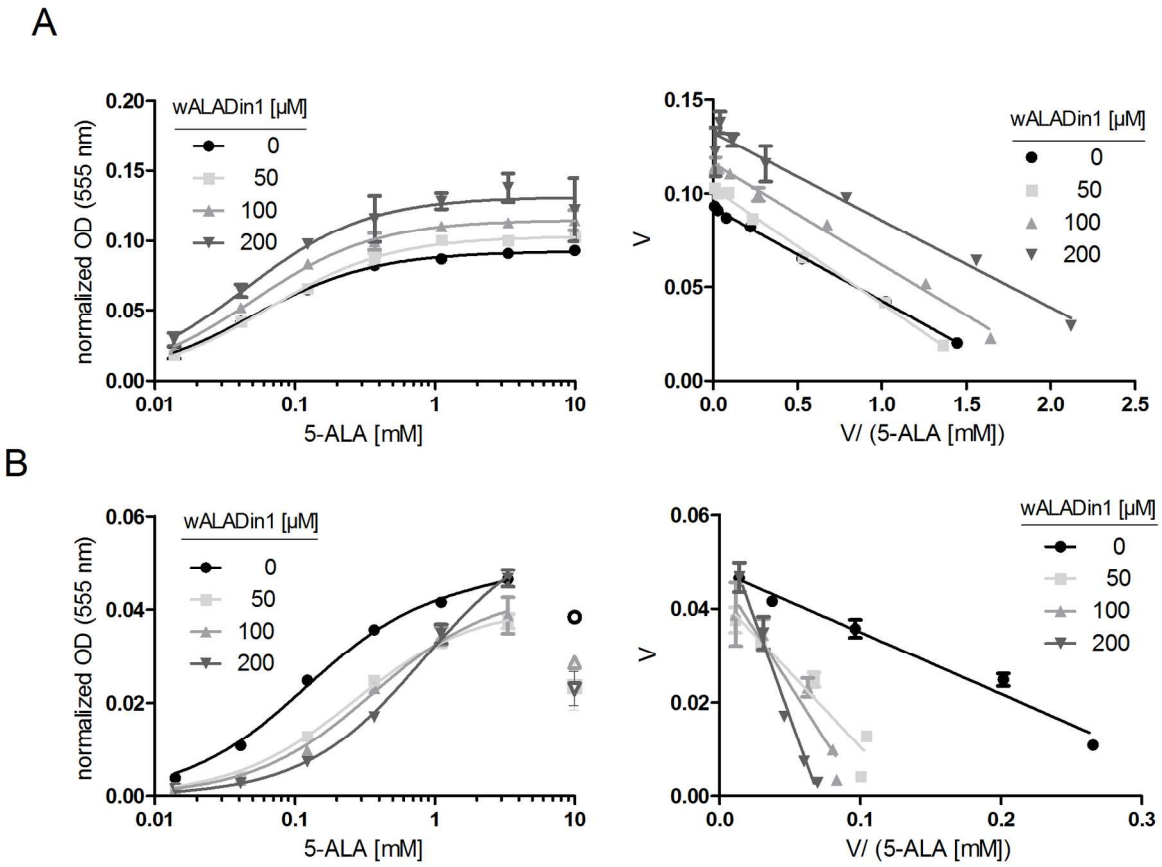

Figure S7. Michaelis-Menten kinetics of *Pa*PBGS. A) Stimulatory (100 mM Tris-HCl pH 8.0, 5 mM 5-ALA, 1 mM $MgCl_2$, 100 mM KCl, if not indicated otherwise). B) Inhibitory conditions (100 mM Tris-HCl pH 7.5, 0.2 mM 5-ALA, 1 mM $MgCl_2$, no KCl). Graphs include 5-ALA dilution series showing curves fit by non-linear regression assuming conventional Michaelis-Menten kinetics (left) and linearized Eadie-Hofstee representation of this data (right). A) Under "standard stimulatory" conditions V_{MAX} increased with increasing concentrations of wALADin1, while K_M was not affected. B) Under "standard inhibitory" conditions a non-canonical progression of the 5-ALA response curve and the linearized Eadie-Hofstee representation was observed. K_M was increased in a concentration-dependent manner while V_{MAX} was decreased at 50 and 100 μM wALADin1, but increased at higher concentrations of wALADin1. [5-ALA] > 10 mM resulted in apparent enzyme inhibition by the substrate, thus the corresponding data points were excluded from the regression analysis. All graphs show means ± SD of triplicates and are representative of two experiments.

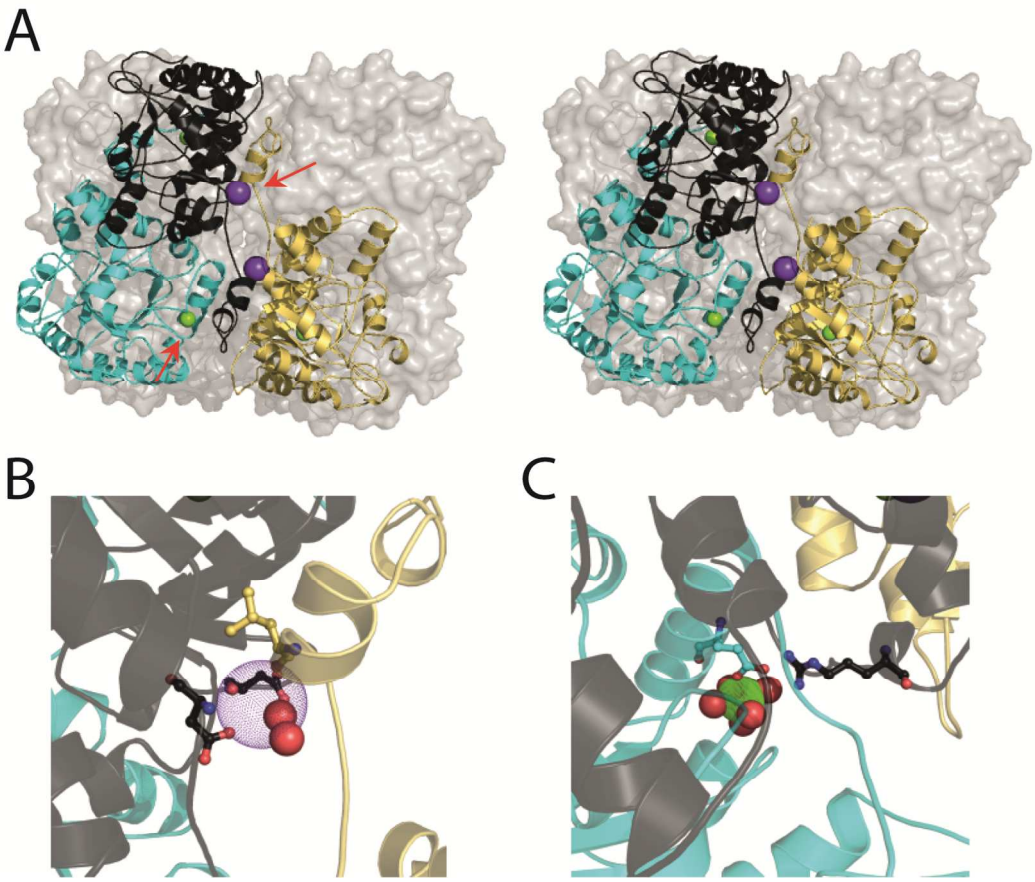

Figure S8. Structural representation of Mg^{2+}- and K^{+}-binding sites in the *Pa*PBGS octamer. (**A)** A stereoview of the *P. aeruginosa* PBGS octamer (PDBid 1GZG) is shown with subunits A, C and D as yellow, cyan and black cartoons and the remaining subunits as grey surfaces. The allosteric magnesium ions of subunits A, C and D are shown as green spheres; the allosteric potassium ions of subunit D are shown as purple spheres. Red arrows indicate the specific potassium and magnesium ions detailed in panels B and C, each of which rotate the molecule slightly to improve visualization. (**B)** The featured potassium ion (purple dots) of subunit D interacts with Asp37 and Asp319 of subunit D, Leu27 of subunit A (residues shown as ball-and-sticks with the carbons colored as in panel A and other atoms in CPK), and two water molecules (shown as red spheres). (**C)** The magnesium ion of subunit C (green dots) interacts with Glu245 of subunit C, five water molecules, with a second coordination sphere interaction to Arg19 of subunit A (shown as described for panels A and B).

Supplementary Methods

Thermal Shift Assay The environmentally-sensitive fluorescent dye Sypro® Orange (Sigma Aldrich, Munich, Germany) was used to monitor the melting curve of the *Pa*PBGS protein as in previous studies.[8-10] The 10 µL reaction mixture contained 5 µM *Pa*PBGS subunit in 100 mM Tris-HCl pH 8.0, 1 mM $MgCl_2$ with or without 100 mM KCl and different concentrations of wALADin1 or DMSO. The protein was denatured in 0.5 °C increments every 30 s from 27 °C to 95 °C and fluorescence (excitation at 470 nm; detection at 510nm) was measured with a RotorGene RG-3000 (Corbett Life Sciences, Qiagen, Hilden, Germany). Melting temperatures (T_m) were determined by first derivative analysis of primary fluorescence data using RotorGene 6 software.

Supplementary References

1. Dereeper, A.; Audic, S.; Claverie J.M., Blanc G. BLAST-EXPLORER helps you building datasets for phylogenetic analysis. BMC Evol. Biol. **2010**, *10*, 8.

2. Dereeper, A.; Guignon, V.; Blanc, G.; Audic, S.; Buffet, S.; Chevenet, F.; Dufayard, J.F.; Guindon, S., Lefort, V.; Lescot, M.; Claverie, J.M.; Gascuel O. Phylogeny.fr: robust phylogenetic analysis for the non-specialist. Nucleic Acids Res. **2008**, *36* (Web Server issue),W465-469.

3. Edgar, R.C. MUSCLE: multiple sequence alignment with high accuracy and high throughput. Nucleic Acids Res. **2004**, *32*, 1792-1797.

4. Castresana, J. Selection of conserved blocks from multiple alignments for their use in phylogenetic analysis. Mol. Biol. Evol. **2000**, *17*, 540-552.

5. Guindon, S.; Gascuel, O. A simple, fast, and accurate algorithm to estimate large phylogenies by maximum likelihood. Syst. Biol. **2003**, *52*, 696-704.

6. Anisimova, M.; Gascuel, O. Approximate likelihood ratio test for branchs: A fast, accurate and powerful alternative. Syst. Biol. **2006**, *55*, 539-52.

7. Chevenet, F.; Brun, C.; Banuls, AL.; Jacq, B.; Chisten, R. TreeDyn: towards dynamic graphics and annotations for analyses of trees. BMC Bioinformatics. **2006**, *7*, 439.

8. Lentz, C. S.; Halls, V.; Hannam, J. S.; Niebel, B.; Strubing, U.; Mayer, G.; Hoerauf, A.; Famulok, M.; Pfarr, K. M. A selective inhibitor of heme biosynthesis in endosymbiotic bacteria elicits antifilarial activity in vitro. Chem. Biol. **2013**, *20*, 177-187.

9. Pantoliano, M. W.; Petrella, E. C.; Kwasnoski, J. D.; Lobanov, V. S.; Myslik, J.; Graf, E.; Carver, T.; Asel, E.; Springer, B. A.; Lane, P.; Salemme, F. R. High-density miniaturized thermal shift assays as a general strategy for drug discovery. J. Biomol. Screen. **2001**, *6*, 429-440.

10. Senisterra, G.; Chau, I.; Vedadi, M. Thermal denaturation assays in chemical biology. Assay. Drug. Dev. Technol. **2012**, *10*, 128-136.